Journal of Alloys and Compounds 502 (2010) 411–416

Contents lists available at ScienceDirect

Journal of Alloys and Compounds

journal homepage: www.elsevier.com/locate/jallcom

Cyclic oxidation and diffusion barrier behaviors of oxides dispersed NiCoCrAlY coatings

Hui Peng, Hongbo Guo*, Jian He, Shengkai Gong*

School of Materials Science and Engineering, Beihang University, No. 37 Xueyuan Road, Beijing, 100191, China

ARTICLE INFO

Article history:
Received 19 January 2010
Received in revised form 20 April 2010
Accepted 25 April 2010
Available online 4 May 2010

Keywords:
Thermal barrier coatings (TBCs)
Diffusion barrier
Inter-diffusion
Oxidation
Electron beam-physical vapor deposition (EB-PVD)

ABSTRACT

NiCoCrAlY has been widely used as the bond coat material in thermal barrier coatings (TBCs). Inter-diffusion between the bond coat and superalloy could degrade the performance of the coating and the mechanical properties of the superalloy. In this paper, oxide dispersed (OD) NiCoCrAlY coatings were deposited onto superalloy DZ 125 using EB-PVD by introducing oxygen during the deposition process. Cyclic oxidation and inter-diffusion behaviors of the coated specimens at 1323 K were investigated. The OD coating deposited with high level oxygen input effectively prevented outward diffusion of the elements such as Hf and W in superalloy. For the conventional NiCoCrAlY coating, Hf migrated to the coating surfaces and caused accelerated thickening and chipping spallation of TGO. The OD coating with high level oxygen input exhibits an improved cyclic oxidation resistance as compared to the conventional NiCoCrAlY coating and the OD coating with lower level of oxygen input.

1. Introduction

Improved efficiency in modern gas turbines is usually achieved by increasing combustion temperature in the combustor sections of the engines. However, high temperature also increases the oxidation and corrosion rate of the metallic components. Thermal barrier coating (TBC) systems, usually consisting of a metallic bond coat (MCrAlY, M = Ni, Co or Ni + Co) and a ceramic topcoat of yttria stabilized zirconia (YSZ), are used to protect the surface of the hot sections against oxidation and corrosion attack [1,2]. More recently, extensive efforts have been made to improve the operation temperature and service life time of TBC systems for further improvement in engine's performance. Novel ceramic candidates, such as $La_2Zr_2O_7$ with pyrochlore structure [3,4] and $La_2Ce_2O_7$ with fluorite structure have been investigated [5]. Also, new processing technologies, such as electrospark deposition, have been used for depositing MCrAlY coatings with high density and good homogeneity [6,7].

Inter-diffusion across the superalloy/coating interface has been observed at elevated temperature. The migration of elements across the interface alters the chemical compositions and microstructures of both the bond coat and the underlying superalloy substrate in the vicinity of the interface [8–10]. For instance, inward diffusion of Al and Cr from the bond coat could degrade the oxidation resistance of the coating [11,12]. Also, outward diffusion of refractory elements such as W, Mo from the superalloy could weaken the adherence of the thermally grown oxide (TGO) as they diffuse into the bond coat, which would accelerate premature spallation failure of TBC [13]. On the other hand, inter-diffusion between the coating and the superalloy may also cause the microstructure instability of the superalloy. Especially, for the advanced Ni-base single crystal superalloys containing high levels of refractory elements such as W, Mo, Re and Ru, inward diffusion of Al from the coating and outward diffusion of Ni from the superalloy could lead to the formation of secondary reaction zones (SRZ) and topologically close packed phase (TCP) in the superalloy. It has been shown that SRZ and TCP lead to a significant reduction in the high-temperature stress–rupture creep resistance of the single crystals [14–16].

Extensive efforts have been made to inhibit the inter-diffusion, such as carburizing or nitriding of the superalloy substrate to form stable carbides or nitrides [17–19]. Other proposed approaches involve diffusion barrier layers, such as TiN layer [20], Al–O–N thin-film layer [21,22], Cr–O–N thin-film layer [22], Re (W)–Cr–Ni layer [23,24] and Ni–W diffusion barrier [15]. Among various diffusion barrier candidates, α-Al_2O_3 is a very effective diffusion barrier material to suppress the inter-diffusion between MCrAlY and superalloy [25,26]. Simultaneously, large thermal stresses, resulting from the thermal expansion mismatch between α-Al_2O_3 and superalloy, would cause cracking of the α-Al_2O_3 layer when the coated superalloy is subjected to thermal cycling loading.

* Corresponding authors. Tel.: +86 10 8231 7117; fax: +86 10 8233 8200.
E-mail addresses: guo.hongbo@buaa.edu.cn (H. Guo), gongsk@buaa.edu.cn (S. Gong).

0925-8388/$ – see front matter © 2010 Elsevier B.V. All rights reserved.
doi:10.1016/j.jallcom.2010.04.183

Recently, oxide dispersion strengthened (ODS) superalloy foils were prepared by advanced electron beam-physical vapor deposition (EB-PVD) technique and revealed excellent mechanical properties [27]. However, there is so far no report on the oxide dispersed (OD) MCrAlY coatings fabricated by EB-PVD and lack of knowledge about the diffusion barrier effect and oxidation resistance of the OD coatings.

In this work, the OD NiCoCrAlY coatings were fabricated via inducing certain amount of oxygen into the vacuum chamber during the deposition process. The microstructure, oxidation and inter-diffusion behaviors of the coating systems were investigated.

2. Experimental

Ni-based directionally solidified (DS) superalloy DZ 125 was used as substrate material, whose nominal composition is shown in Table 1. The rectangular specimens (15 mm × 10 mm × 3 mm) were cut from the superalloy rod by wire-cutting. Prior to deposition, all specimen surfaces were ground with SiC paper, followed by sand blasting and ultrasonic bath cleaning with alcohol and acetone.

Three kinds of coatings were produced as follows: (1) conventional EB-PVD NiCoCrAlY coating, designed as A; (2) OD NiCoCrAlY coating (O_2: 100 sccm), designed as B, (3) OD NiCoCrAlY coating (O_2: 300 sccm), designed as C. The actual composition of the NiCoCrAlY coating is Ni–20Co–22Cr–8.80Al–1.46Y (in wt.%). All the coatings were produced under the same deposition condition. One EB gun was used to evaporate the NiCoCrAlY target, the power for which was up to 30 kW. The specimens were heated with another EB gun to keep the substrate temperature at 1123 K during the deposition. An oxygen jet was linked to the EB-PVD facility to provide oxygen input during deposition of the NiCoCrAlY coatings. The conventional NiCoCrAlY coatings were deposited to a thickness of about 50 μm. For processing the OD coatings, a thin NiCoCrAlY layer was firstly deposited onto the superalloy and then oxygen was introduced to the specimen surfaces without interrupting deposition of NiCoCrAlY. The flow rate of oxygen was set to be 100 and 300 sccm for coatings B and C, respectively. The flow rate of oxygen was determined based on the evaporation rate of each element in the target, so as to obtain pure Al_2O_3 phase as the selective oxidation product. The introduced oxygen reacted completely with the metallic vapor and had no significant influence on the working pressure. After 3 min, the oxygen jet was closed, while the evaporation and deposition of NiCoCrAlY coatings continued. To identify the phase constituents of the OD zone, the specimens coated with only OD layer were also produced without continuous deposition of NiCoCrAlY coating. After deposition, the coated specimens were annealed at 1323 K in vacuum for 4 h, with a pressure of about 3×10^{-3} Pa.

Cyclic oxidation tests of the coated specimens were performed in a muffle furnace equipped with an automation system that allows the specimens moving in and out automatically. The coated specimens were held in alumina crucibles at 1323 K in the furnace for 50 min, and then were moved out, followed by forced air cooling for 10 min. The weights were recorded by an electronic balance (Sartorious CPA 225D, Germany) with a precision of 10^{-5} g. The measured weight included both the weights of the samples and the spalled oxides.

The microstructures of the coated specimens were characterized by a QUANTA 600 scanning electron microscope (SEM, FEI, Holland) equipped with energy dispersive spectroscopy (EDS) and back scattering electron (BSE) detector. The chemical compositions were determined by electron probe micro-analyzer (EPMA, JXA-8100). The phase constituents of the thermally grown oxides (TGO) on the coatings were identified by X-ray diffraction (XRD) using Cu K_α radiation.

3. Results and discussion

3.1. Microstructures of OD coatings

The XRD patterns of the specimens coated with only OD layer are shown in Fig. 1. Only the peaks of γ and γ′ phases were detected in the as-deposited specimen, meanwhile, α-Al_2O_3 phase was also identified after 4 h annealing at 1323 K. This implies that the transition of the oxides in the OD zone from amorphous alumina to α-Al_2O_3 occurred during the vacuum annealing at 1323 K [28].

Fig. 2 shows the cross-sections of SEM micrographs of the as-deposited coatings. All the coatings reveal nearly the same thickness of 50 μm. The OD coatings consist of three zones: top zone, OD zone and bottom zone. The OD zone and the bottom zone of NiCoCrAlY have nearly the same thickness of 3 μm (Fig. 2b and c). In coating C (higher oxygen input), the OD zone (Fig. 2c) is slightly darker than that of coating B (lower oxygen input) (Fig. 2b), suggesting a higher content of oxides.

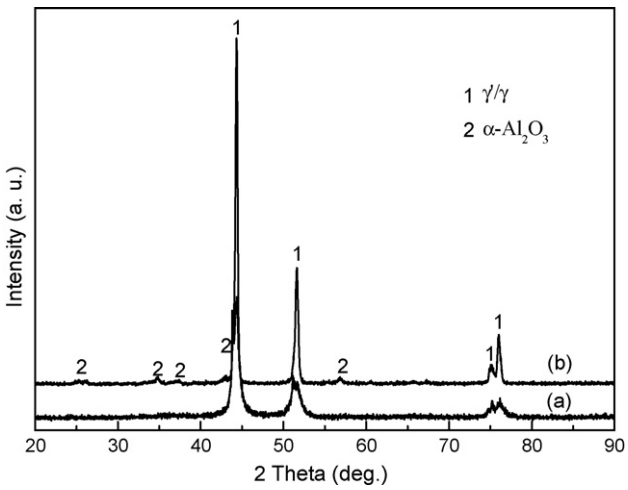

Fig. 1. XRD patterns of the specimen only coated with OD layer before (a) and after annealing at 1323 K in vacuum for 4 h (b).

3.2. High-temperature oxidation behavior

Fig. 3a and b shows the kinetic curves of the coated specimens during cyclic oxidation at 1323 K. Coatings A and B yielded weight gains of 0.82 and 0.74 mg/cm^2 after 160 h, respectively, while coating C yielded a weight gain of 0.53 mg/cm^2 (Fig. 3a). This indicates that coating C showed lower oxidation rate than coatings A and B. The oxidation constant K_p was determined based on the Wagner equation. The oxidation kinetics of all the coatings followed the parabolic law. However, the calculated value of K_p for the conventional coating is about 8×10^{-7} mg^{-2} cm^{-4} s^{-1}, which is very close to that for coating B, as shown in Fig. 3b. The value for coating C is 2.9×10^{-7} mg^{-2} cm^{-4} s^{-1}, which is only half of those of coatings A and B. From this result, it can be concluded that coating C exhibits better oxidation resistance than coatings A and B.

Fig. 4a–c shows the back scattering images (BSI) of cross-sections of the coatings after 160 h oxidation. Thermally grown oxide (TGO) layers can be seen on the coatings. Among the three coatings, coating B reveals a little thicker TGO, meanwhile, chipping spallation of the TGO occurred in coating A. Besides, a large amount of internal oxide pegs (in bright) are presented in the TGO of coatings A and B. The oxide pegs are identified by EPMA as Hf-rich oxides. It can be inferred that Hf diffused from the superalloy substrate to the coating surface during high-temperature oxidation. In contrast to coatings A and B, coating C exhibits a dense and continuous oxide layer. Little Hf-rich oxide is observed in the TGO, instead, Y-rich oxides (light grey particles) are enclosed in the TGO.

From the surface morphologies of the coatings as shown in Fig. 5a, it is further proved that chipping spallation of the TGO occurred in the conventional coating, while coating C shows a dense and perfect oxide appearance even after 160 h cyclic oxidation (Fig. 5b).

Table 1
Compositions of directionally solidified superalloy DZ 125 (in wt.%).

C	Cr	Co	W	Mo	Al	Ti	Ta	Hf	Ni
< 0.12	8.4–9.4	9.5–10.5	6.5–7.5	1.5–2.5	4.8–5.4	0.7–1.2	3.5–4.1	1.2–1.8	Balance

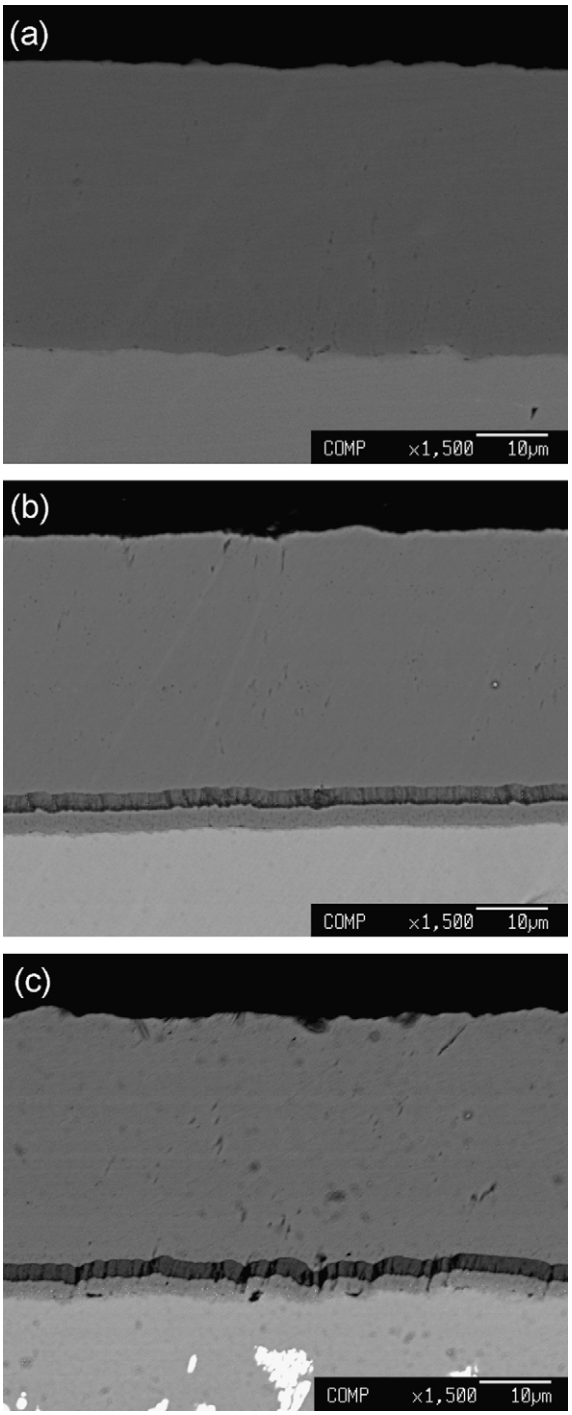

Fig. 2. Cross-sections images of the as-deposited coatings: (a) NiCoCrAlY; (b) OD NiCoCrAlY (100 sccm); (c) OD NiCoCrAlY (300 sccm).

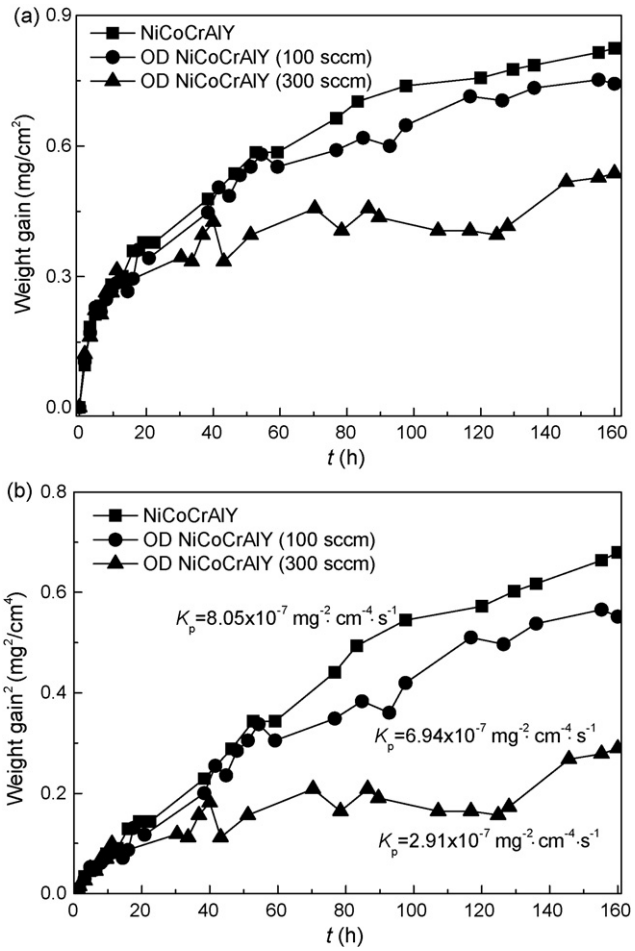

Fig. 3. Weight gain (a) and its square (b) after cyclic oxidation of coatings at 1323 K for 160 h.

Phases of the oxides grown on the coatings were identified by XRD, as shown in Fig. 6. For all the coatings, α-Al_2O_3 phase is the major phase in the TGO. Besides, an amount of HfO_2 and $Y_2Hf_2O_7$ phases were also detected in the TGO of coating A. However, only $Y_2Hf_2O_7$ phase was detected in the TGO of coating B. This confirms that the Hf-rich oxides presented in Fig. 4a and b mainly comprise HfO_2 and $Y_2Hf_2O_7$. The absence of HfO_2 in coating B implies a lower Hf concentration. Note that HfO_2 and $Y_2Hf_2O_7$ phases were not detected in the TGO of coating C, instead, $YAlO_3$ phase was detected.

Based on the above results, it can be inferred that inter-diffusion between the NiCoCrAlY coating and the underlying superalloy DZ 125 occurred during high-temperature oxidation. Quite an amount of Hf diffused from the superalloy to the coating surface. As a consequence, Hf-rich oxides such as HfO_2 and $Y_2Hf_2O_7$ were enriched in the TGO of coatings A and B, which could be a reason for the higher oxidation rate of the NiCoCrAlY coating. Compared to coatings A and B, coating C exhibited an improved cyclic oxidation resistance, possibly due to that the OD zone formed in coating C effectively blocked outward diffusion of the elements such as Hf from the superalloy.

It has been reported that the addition of reactive elements (Hf, Dy, et al.) to MCrAlY or NiAl coatings is helpful to improve oxidation resistance of the coatings [29–31]. Minor Hf (less than 0.5 at.%) can not only reduce the growth rate of TGO but also improve the adherence of the oxide scale. However, excessive Hf can accelerate TGO thickening, finally causing spallation of oxide scale by over-doping effect [9]. On the other hand, the addition of small amount of Y in the NiCoCrAlY coating also contributes to enhance the scale adherence by pegging mechanism [32–34].

3.3. Diffusion barrier behavior

The element distributions along the thickness of the coated specimens after 160 h oxidation at 1323 K were analyzed by EPMA and the elements depth profiles are depicted in Fig. 7. Enrichment of Al occurs in the surface layers, due to the presence of Al_2O_3 in the TGO, as proved by XRD results in Fig. 6. Besides, Al is also enriched in the OD zones of coatings B and C since the OD zones basically consist of Al_2O_3, as a result of selective oxidation.

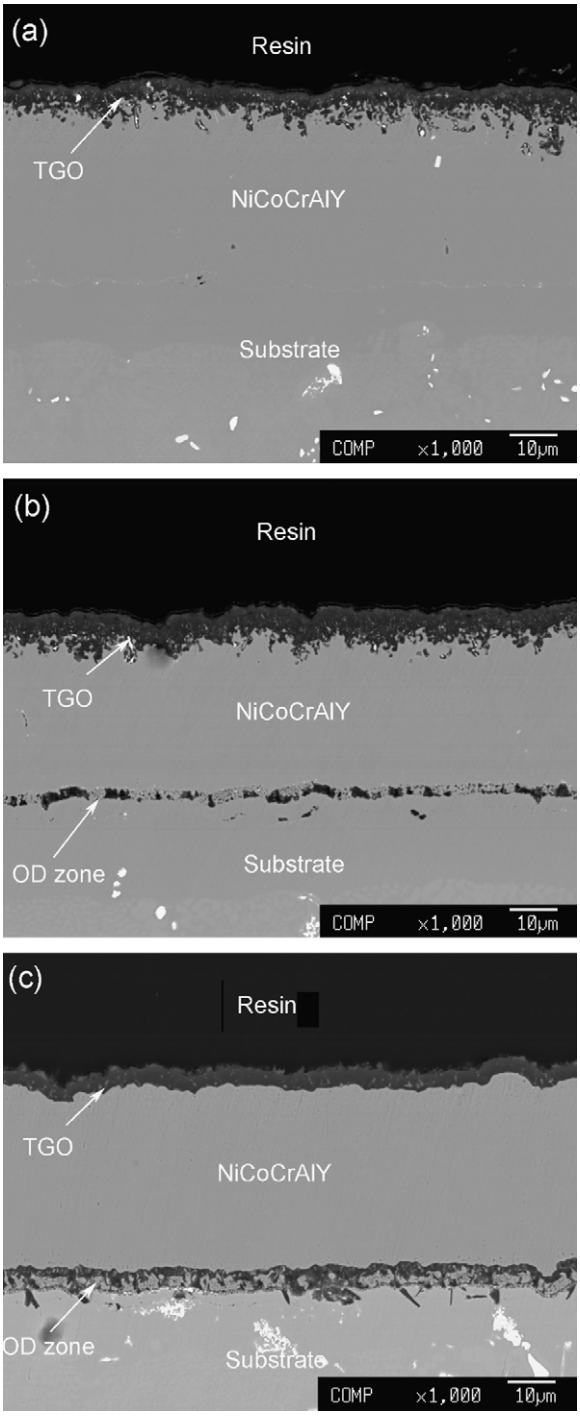

Fig. 4. Cross-sections of coatings after oxidation at 1323 K for 160 h (a) NiCoCrAlY; (b) OD NiCoCrAlY (100 sccm); (c) OD NiCoCrAlY (300 sccm).

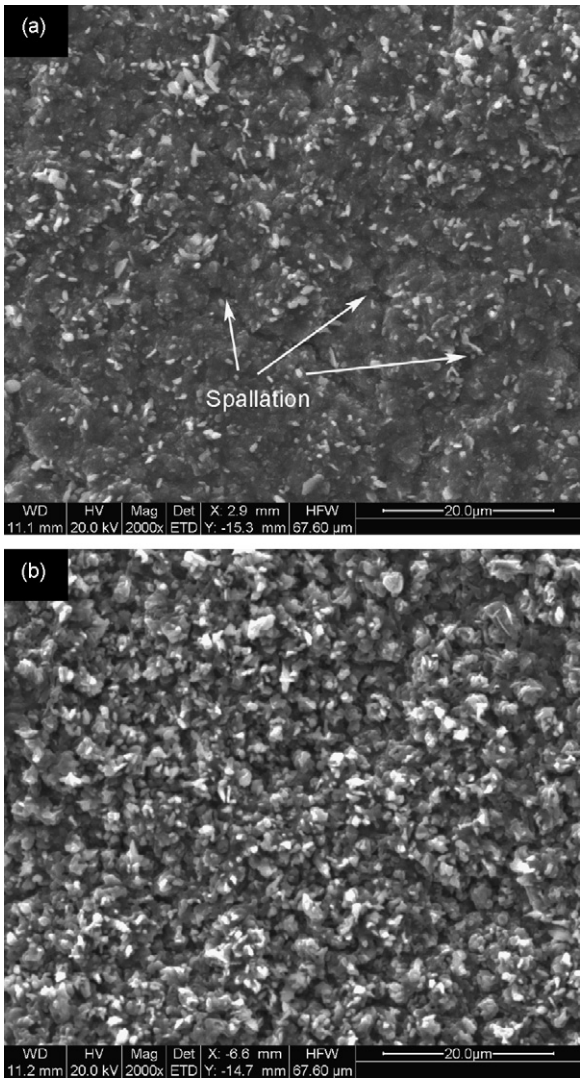

Fig. 5. Surface morphologies of coatings after oxidation at 1323 K for 160 h (a) NiCoCrAlY; (b) OD NiCoCrAlY (300 sccm).

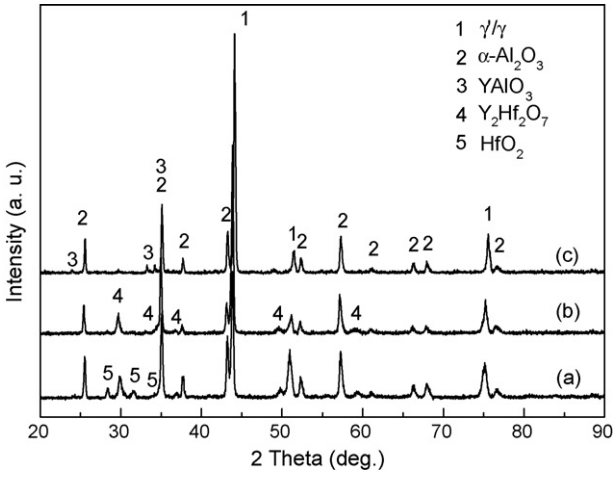

Fig. 6. XRD patterns of coatings after oxidation at 1323 K for 160 h (a) NiCoCrAlY; (b) OD NiCoCrAlY (100 sccm); (c) OD NiCoCrAlY (300 sccm).

In coatings A and B, an amount of W, Ti and Ta is presented in the coating zone, due to outward diffusion of these elements from the underlying superalloy. However, there are no traces of the above elements in coating C despite these elements are enriched beneath the OD zone. It is clear that the OD zone in coating C effectively blocked outward diffusion of these elements. W and Ta are refractory elements usually used for improving the high-temperature strength of superalloys. The loss of these elements in the superalloy DZ125, due to the outward diffusion as shown in Fig. 7a and b, could degrade the desired strength of the superalloy. On the other hand, the presence of W, Ti and Ta in the coatings could be harmful to the

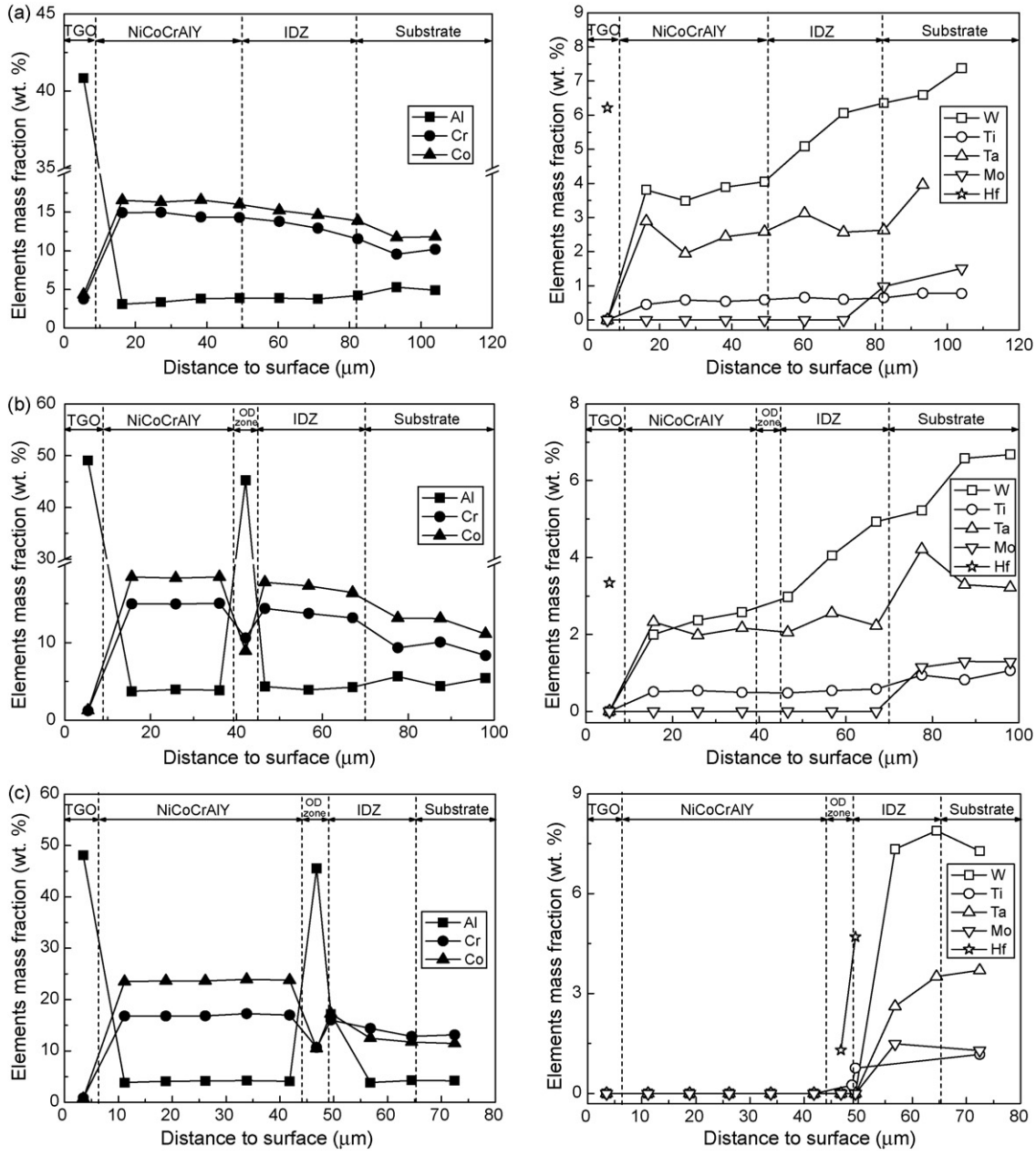

Fig. 7. Element distributions across the thickness of the coated specimens after oxidation at 1323K for 160 h: (a) NiCoCrAlY; (b) OD NiCoCrAlY (100 sccm); (c) OD NiCoCrAlY (300 sccm).

oxidation resistance of the coatings. It has been shown that voids formed beneath the TGO layer due to volatilization of WO_3 at high temperatures could weaken the oxide scale adherence [35,36].

About 6 and 4 wt.% Hf were detected in the TGO layers of coatings A and B, respectively, as a result of outward diffusion. As shown in Fig. 6, Hf-rich oxides were presented in the TGO layers in the form of HfO_2 and $Y_2Hf_2O_7$. There is no trace of Hf in the TGO layer in coating C, however, about 4.7 wt.% Hf was detected beneath the OD zone. This gives the evidence that outward diffusion of Hf was blocked by the OD zone and as a result, Hf was enriched in the area beneath the OD zone. Like W and Ta, Hf is also a strengthening element in the superalloy. The loss of Hf could also degrade the strength of the superalloy. The OD zone in coating C worked as a diffusion barrier between the coating and superalloy and thus prevented outward diffusion of the refractory elements. Therefore, the OD zone is beneficial to sustain the strength of the superalloy. On the other hand, as discussed earlier, in the case of coatings A and B, excessive Hf caused accelerated thickening and finally spallation of TGO by so-called over-doping effect. As for coating C, the $YAlO_3$ pegs improved the oxide scale adherence. Consequently, the coating exhibits an improved cyclic oxidation resistance as compared to coatings A and B.

Note that the OD zone formed in coating B with a lower level of oxygen input could not effectively block outward diffusion of Hf, Ti, Ta and W from the superalloy. One of explanations is that the diffusion barrier effect of the OD zone is dependent on the distribution, contents and grain size of Al_2O_3 phase in the OD zone. In the case of coating B, the content of Al_2O_3 in the OD zone is not high enough to form a diffusion barrier. Furthermore, the distribution of Al_2O_3 is not homogeneous. Thus, coating B could not effectively prevent refractory elements from outward diffusion. It should also be noted that a pure Al_2O_3 layer is not desirable to work as a diffusion barrier layer. In this case, Al_2O_3 is very brittle and its thermal expansion coefficient is relatively lower than those of NiC-

oCrAlY bond coat and substrate superalloy. During thermal cycling, high stress concentration would occur in the Al_2O_3 layer, eventually leading to cracking of the layer and spallation failure of TBCs. For coating C, the OD zone effectively blocked outward diffusion of elements from the superalloy. Consequently, the coating exhibited an enhanced oxide scale adherence and excellent cyclic oxidation resistance.

4. Conclusions

Oxide dispersed (OD) NiCoCrAlY coatings were prepared using EB-PVD method by introducing oxygen during deposition of the NiCoCrAlY coatings. The OD coating deposited with high level oxygen input (coating C) effectively prevented outward diffusion of the elements from the superalloy such as Hf and W. For the conventional coating, Hf diffused to the coating surface and led to chipping spallation of TGO by over-doping effect. The OD coating deposited with high level oxygen input exhibited an improved cyclic oxidation resistance as compared to the conventional NiCoCrAlY coating and the OD coating deposited with lower level of oxygen input.

Acknowledgements

This research is sponsored by the New Century Excellent Talents in University (NCET) and National Nature Science Foundations of China (NSFC, no. 50771009 and no. 50731001).

References

[1] N.P. Padture, M. Gell, E.H. Jordan, Science 296 (5566) (2002) 280–284.
[2] T.R. Kakuda, A.M. Limarga, T.D. Bennett, D.R. Clarke, Acta Mater. 57 (8) (2009) 2583–2591.
[3] Z.H. Xu, L.M. He, R. Mu, S.M. He, X.Q. Cao, J. Alloys Compd. 492 (1–2) (2010) 701–705.
[4] Z.H. Xu, L.M. He, R.D. Mu, X.H. Zhong, Y.F. Zhang, J.F. Zhang, X.Q. Cao, J. Alloys Compd. 473 (1–2) (2009) 509–515.
[5] W. Ma, H.Y. Dong, H.B. Guo, S.K. Gong, Surf. Coat. Technol. (2010), doi:10.1016/j.surfcoat.2010.03.053.
[6] Y.J. Xie, M.C. Wang, J. Alloys Compd. 480 (2) (2009) 454–461.
[7] Y.J. Xie, M.C. Wang, J. Alloys Compd. 484 (1–2) (2009) 21–24.
[8] T.N. Rhys-Jones, Corros. Sci. 29 (6) (1989) 623–646.
[9] U. Schulz, M. Menzebach, C. Leyens, Y.Q. Yang, Surf. Coat. Technol. 146 (2001) 117–123.
[10] O. Knotek, E. Lugscheider, F. Loffler, W. Beele, Surf. Coat. Technol. 68–69 (1994) 22–26.
[11] J.R. Nicholls, N.J. Simms, W. Chan, H.E. Evans, Surf. Coat. Technol. 149 (2–3) (2002) 236–244.
[12] A. Hesnawi, H.F. Li, Z.H. Zhou, S.K. Gong, H.B. Xu, Vacuum 81 (8) (2007) 947–952.
[13] J. Muller, D. Neuschutz, Vacuum 71 (1–2) (2003) 247–251.
[14] W.S. Walston, J.C. Schaeffer, W.H. Murphy, in: R.D. Kissinger (Ed.), Superalloys, TMS, 1996, pp. 9–18.
[15] E. Cavaletti, S. Naveos, S. Mercier, P. Josso, M.P. Bacos, D. Monceau, Surf. Coat. Technol. 204 (6–7) (2009) 761–765.
[16] A. Sato, H. Harada, K. Kawagishi, Metall. Mater. Trans. A 37A (3) (2006) 789–791.
[17] J.C. Schaeffer, U.S. Patent 5334263 (1994).
[18] K.S. O'hara, W.S. Walston, J.C. Schaeffer, U.S. Patent 6447932 (2002).
[19] I.E. Locci, R.A. Mackay, A. Garg, F. Ritzert, NASA, NASA/TM-2004-212920, 2004.
[20] M. Uunonen, P. Kettunen, in: A. Strang (Ed.), Fifth International Charles Parsons Turbine Conference, Churchill College, Cambridge, UK, 2000, pp. 724–732.
[21] R. Cremer, M. Witthaut, K. Reichert, M. Schierling, D. Neuschutz, Surf. Coat. Technol. 109 (1–3) (1998) 48–58.
[22] Q.M. Wang, Y.N. Wu, M.H. Guo, P.L. Ke, J. Gong, C. Sun, L.S. Wen, Surf. Coat. Technol. 197 (1) (2005) 68–76.
[23] M. Sakata, S. Hayashi, T. Nishimoto, T. Yoshioka, T. Narita, Oxid. Met. 68 (5–6) (2007) 295–311.
[24] D. Sumoyama, K.Z. Thosin, T. Nishimoto, T. Yoshioka, T. Izumi, S. Hayashi, T. Narita, Oxid. Met. 68 (5–6) (2007) 313–329.
[25] J. Muller, M. Schierling, E. Zimmermann, D. Neuschutz, Surf. Coat. Technol. 121 (1999) 16–21.
[26] W.Z. Li, Y.Q. Li, Q.M. Wang, C. Sun, X. Jiang, Corros. Sci. 52 (5) (2010) 1753–1761.
[27] X.D. He, Y. Xin, M.W. Li, Y. Sun, J. Alloys Compd. 467 (1–2) (2009) 347–350.
[28] S.K. Jha, Y.H. Sohn, S. Sastri, N. Gunda, J.A. Haynes, Surf. Coat. Technol. 183 (2–3) (2004) 224–232.
[29] U. Schulz, K. Fritscher, A. Ebach-Stahl, Surf. Coat. Technol. 203 (5–7) (2008) 449–455.
[30] H.L. Wu, H.B. Guo, S.K. Gong, J. Alloys Compd. 492 (1–2) (2010) 295–299.
[31] H.B. Guo, X.Y. Wang, J. Li, S.X. Wang, S.K. Gong, Trans. Nonferrous. Met. Soc. China 19 (5) (2009) 1185–1189.
[32] R. Cueff, H. Buscail, E. Caudron, F. Riffard, C. Issartel, S. El Messki, Appl. Surf. Sci. 229 (1–4) (2004) 233–241.
[33] T.J. Nijdam, W.G. Sloof, Acta Mater. 55 (17) (2007) 5980–5987.
[34] A. Gil, D. Naumenko, R. Vassen, J. Toscano, M. Subanovic, L. Singheiser, W.J. Quadakkers, Surf. Coat. Technol. 204 (4) (2009) 531–538.
[35] D.B. Zhang, S.K. Gong, H.B. Xu, Z.Y. Wu, Surf. Coat. Technol. 201 (3–4) (2006) 649–653.
[36] B.A. Pint, Oxid. Met. 49 (5) (1998) 531–559.